nature biotechnology

PERSPECTIVE

Toward fluorescence nanoscopy

Stefan W Hell

For more than a century, the resolution of focusing light microscopy has been limited by diffraction to 180 nm in the focal plane and to 500 nm along the optic axis. Recently, microscopes have been reported that provide three- to sevenfold improved axial resolution in live cells. Moreover, a family of concepts has emerged that overcomes the diffraction barrier altogether. Its first exponent, stimulated emission depletion microscopy, has so far displayed a resolution down to 28 nm. Relying on saturated optical transitions, these concepts are limited only by the attainable saturation level. As strong saturation should be feasible at low light intensities, nanoscale imaging with focused light may be closer than ever.

In 1873, Ernst Abbe discovered that the resolution of a focusing light microscope is limited by diffraction[1]. This physical insight became one of the most prominent paradigms in the natural sciences, with paramount importance in biology. Although the advent of confocal and multiphoton fluorescence microscopes facilitated three-dimensional imaging, they did not really improve the resolution[2–4]. In the best case, these and other established focusing microscopes resolve 180 nm in the focal plane (x,y) and only 500–800 nm along the optic axis (z)[5].

Fluorescence microscopes routinely detect single molecules if their fellow molecules are far enough apart[6]. By the same token, they discern several molecules at arbitrary distance, provided none of them is of the same kind. Telling apart fluorescent labels that are spectrally distinct is not challenged by diffraction. Therefore, resolution must be confused neither with single-molecule sensitivity[7] nor with measuring of distances between distinct fluorescent markers[8–12]. Notwithstanding the importance of these issues, this review is concerned with improving the ability of a light microscope to distinguish identical fluorescent items at high spatial density, such as the distribution of a green fluorescent protein (GFP) fusion protein in a cell. Likewise, it is concerned with methods for producing fluorescent volumes that are fundamentally smaller than those of confocal and multiphoton microscopy. The approaches discussed rely on visible light and regular objective lenses. Moreover, they are designed for operation at 18–37 °C and are applicable to the imaging of live cells.

According to diffraction theory, the resolution of a focusing light microscope is related to the size of its focal spot. The spot size can be decreased by using shorter wavelengths and larger aperture angles[1,13] (**Box 1**), but this strategy has the shortcoming that wavelengths $\lambda < 350$ nm are incompatible with live cell imaging and the lens half-aperture is technically limited to 70°. The restricted aperture angle is also responsible for the poorer resolution along the optic axis. Therefore, during the past decade, concepts have appeared for improving the axial resolution[14–16] by combining the aperture of opposing lenses. The up to sevenfold-improved axial sectioning capability of these techniques, termed 4Pi microscopy[17,18] and I^{5}M microscopy[19], should be a strong incentive to map organelles, the nucleus and protein distributions at higher resolution.

The notion of the virtually insurmountable diffraction barrier stems from the fact that focusing always results in a blurred spot of light. Consequently, near-field optical microscopes abandon focusing altogether[20]. To localize the interaction of the light with the object to subdiffraction dimensions, near-field microscopes use ultrasharp tips or tiny apertures that confine imaging to surfaces. Consequently, this approach does not allow the noninvasive imaging of live cells.

Defeating the resolution limit without defeating diffraction per se is evidently preferable. Although this formidable problem has challenged many physicists[21,22], feasible proposals did not emerge in the past. Nevertheless, it had long been clear that the crossing of the diffraction barrier would be enabled by a nonlinear relationship between the intensity of the illumination light and the signal to be measured. Such a nonlinear relationship is offered by the fluorescence induced by m-photon absorption (see article by Webb, this issue), which has led to the long-standing popular notion that superresolution is readily attained by the cooperative absorption of many photons. But as we now know, m-photon excitation ($m > 1$) of a fluorophore has not opened up the nanoscale yet and is unlikely to do so in the future. Although it is true that m-photon absorption occurs mainly at the center of the spot, the concomitant narrowing of the effective spot is spoiled by the fact that m-photon excitation usually entails photons of m times lower energy (that is, m times longer wavelength) and thus m times larger focal spots to begin with. In addition, this approach requires very high intensities[23]. Therefore, my collaborators and I[24–26] devised m-photon excitation concepts for working at lower intensities and without photon-energy subdivision, but they rely on very specific fluorophores. Moreover, in spite of being higher than with standard m-photon excitation, the resolution promised by these concepts is still modest.

It was not until the mid 1990s that the first viable concepts to break the diffraction barrier appeared[27,28]. They all share a common principle, that is, the spatially modulated and saturable transition between two molecular states. This principle establishes a whole family of methods for achieving nanoscale resolution in all directions[29–31]. Although the full potential of these approaches remains to be explored, their fundamental nature, pertinence to biotechnology and potential synergy with protein engineering make their review timely. Moreover, recently reported results demonstrate that considerable

Max-Planck-Institute for Biophysical Chemistry, Department of NanoBiophotonics, Am Fassberg 11, 37077 Göttingen, Germany. Correspondence should be addressed to S.W.H. (hell@nanoscopy.de).

Published online 31 October 2003; doi:10.1038/nbt895

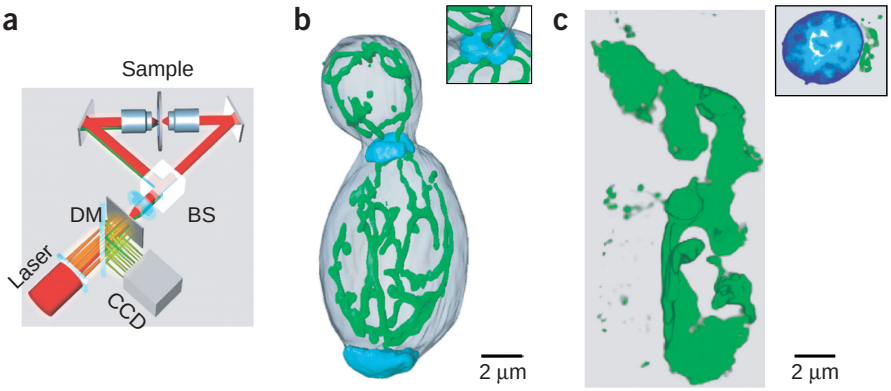

Figure 1 Examples of 4Pi confocal microscopy. (**a**) MMM-4Pi microscopy for live cell imaging. The sample is placed between two opposing water-immersion lenses that are jointly used for multiphoton excitation with up to 64 pairs of 4Pi spots. These spots are produced by splitting an array of pulsed laser beamlets at the beamsplitter (BS). The 4Pi focal array is brushed across the specimen by fast scanning (not shown). Fluorescence from the spots is imaged onto a charge-coupled device (CCD) camera, after being deflected by a dichroic mirror (DM). The system provides fourfold improved sectioning over a comparable confocal microscope. Nonlinear image restoration results in ~100-nm three-dimensional resolution. Recording times, currently ~100 s per $20 \times 20 \times 5$ μm stack, are determined by sample brightness and will be decreased by emerging new CCD camera technology (sketch slightly simplified). (**b**) GFP-labeled mitochondrial compartment of live *Saccharomyces cerevisiae*. The organelle displays strong tubular ramification of a single large body that is exclusively located beneath the plasma membrane (counterstained in blue). Inset, a mitochondrial tubule that can be followed through the thickened cell wall at the budding site. (**c**) Golgi apparatus, as represented by GalTase-EGFP expression in a live *Vero* cell[44]. Note the convoluted structure of the Golgi apparatus, featuring ribbons and fractionated stacks, as well as smaller tubular and vesicular subcompartments. Inset, an epifluorescence overview image of the same cell, which colocalizes the organelle with the nucleus counterstained in blue. (Data in **a** and **b** are adapted from ref. 18; data in **c** reprinted by permission of *J. Struct. Biol.* from ref. 44.)

progress is being made, such as the first demonstration of spatial resolution of λ/25 with focused light and with regular lenses[32].

In this article, I outline strategies, implementations and initial applications of superresolution microscopy, and finally discuss a potential road map toward imaging with nanoscale resolution in live cells. Bridging the gap between electron and current light microscopy, a 'nanoscope' working with focused light should be a powerful tool for unraveling the relationship between structure and function in cell biology.

Axial resolution improvement with two lenses

Conventional and confocal microscopy fail in distinguishing objects that are more closely stacked than 500–800 nm because the focal spot of a lens is at least three- to fourfold longer than it is wide[3,5,13]. An explanation is that the focusing angle of a lens is not a full solid angle of 4π. If it were, the focal spot would be spherical and the axial resolution as good as its lateral counterpart. Therefore, an obvious way to decrease the axial spot size is to enlarge the focusing angle of the system by synthesizing a larger wavefront with two opposing lenses[14–16].

Wavefront synthesis requires the addition of wave amplitude and phase (that is, interference). A first effort to exploit interference for axial resolution improvement with flat standing waves[33] was limited to 200-nm-thin samples[34], and thus it was not until the advent of spot-scanning 4Pi confocal[14,17] and widefield I^{5}M microscopy[16] that the use of interference led to improved axial resolution in three-dimensional imaging[19,35,36]. The reason is that, while interference readily gives a focal spot of ~$\lambda/4n$ width, it also spawns off periodic side-lobes at ~$\lambda/2n \approx 200$ nm distance, which increase in height and number with decreasing aperture angle[15,33]. Therefore this concept requires focused wavefronts of high-angle lenses[15,37]. Although accurate alignment of two lenses did initially pose challenges, the real physical problem in the development of this concept was avoidance of lobe-induced artifacts.

To solve this problem, three lobe-suppression mechanisms were introduced: first, confocalization[14,15]; second, two-photon excitation[17]; and third, use of excitation/fluorescence wavelength disparities[15–17]. The last of these is particularly efficient if both wavefront pairs are brought to interfere in the sample and at the detector[15,16], respectively, because the respective side-lobes no longer coincide in space. A single mechanism may be sufficient; so far, however, the implementation of at least two mechanisms has proved to be more reliable. After an initial demonstration[35], my laboratory first applied superresolved axial separation with two-photon 4Pi-confocal microscopy to fixed cells[36]. The images can be further augmented by applying nonlinear restoration[38–40], which under biological imaging conditions typically improves the resolution up to a factor of 2 in both transverse and axial directions. Therefore, in combination with image restoration, two-photon 4Pi confocal microscopy has resulted in a resolution of ~100 nm in all directions, as first demonstrated in images obtained by my group of filamentous actin[36] and immunofluorescently labeled microtubules[41,42] in mouse fibroblasts.

Recently, my colleagues and I have introduced a multifocal variant, termed MMM-4Pi[18], enabling 100-nm three-dimensional resolution to be translated into live cell imaging[43]. This method has provided superior three-dimensional images of the reticular network of GFP-labeled mitochondria in live budding yeast cells (**Fig. 1**). Cell-induced phase changes have proved more benign than anticipated[18], but they are likely to confine these methods to the imaging of individual cells or thin cell layers. The deep modulation of the focal spot resulting from the joint action of multiphoton excitation and interference provides a new tool to measure thicknesses of cellular constituents in the 50- to 500-nm range with a precision of a few nanometers[18]. This property has been used to detect changes of ~20 nm in the diameter of mitochondrial tubules on a change of growth conditions[18].

4Pi confocal microscopy requires the sample to be mounted between two coverslips, unless one of the lenses is a dipping lens. The recent development of sample chambers with appropriate air and CO_2 conditions has allowed cell viability to be sustained over periods up to 48 h and enabled 4Pi imaging in live mammalian cells[44]. By imaging the Golgi-resident proteins uridinyl-diphosphate-galactosyltransferase and heparan sulfate-2-*O*-sulfotransferase as enhanced GFP (EGFP) fusion proteins, this work has enabled the first three-dimensional representation of the Golgi apparatus of a live mammalian cell at ~100 nm resolution in all directions (**Fig. 1c**). The results indicate that ~100-nm three-dimensional resolution can be obtained in the imaging of protein distributions in the cytosol and probably also in the nucleus. Extending the technique to multicolor detection will improve the microscope's ability to axially colocalize differently tagged proteins

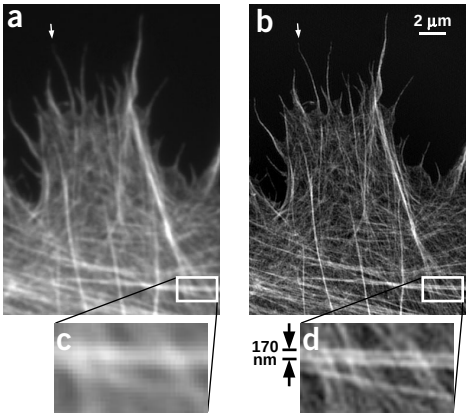

Figure 2 Actin cytoskeleton at the rim of a HeLa cell. (**a**,**b**) Imaged by conventional epifluorescence (**a**) and structured illumination microscopy supported by linear deconvolution (**b**). (**c**,**d**) Insets show the difference in definition possible in **a** and **b**, respectively. Whereas **a** and **c** have a lateral resolution of 280–300 nm, the superresolved images in **b** and **d** have a resolution of 110–120 nm. Note the clear separation of two parallel fibers at 170 nm distance. (Data reprinted by permission of *J. Microsc.* from ref. 48.)

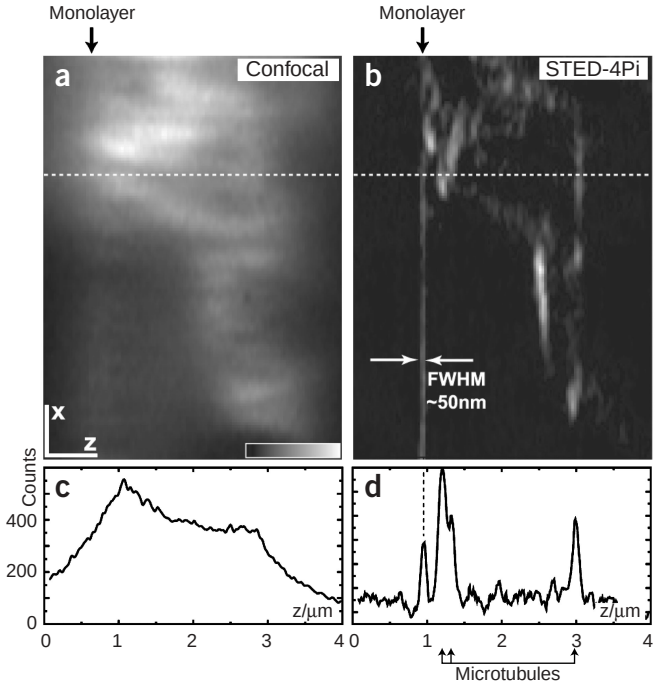

Figure 3 Optical sections from the microtubular network of a human embryonic kidney cell labeled by immunofluorescence. (**a**,**b**) Standard confocal (**a**) and STED-4Pi *xz* sections (**b**) from the same site. The straight vertical line serving as a resolution reference stems from a monomolecular fluorescent layer on the coverslip. The STED-4Pi image was linearly filtered to remove the effect of side-lobes. Note the fundamentally improved clarity in **b**. (**c**,**d**) Profiles of the image data along the marked lines, quantifying an ~15-fold improved axial resolution of the STED-4Pi microscope over its confocal counterpart. The profiles of the microtubules (FWHM 60–70 nm) are broader than the response to the monolayer (~50 nm). The STED-4Pi microscope can distinguish spatially dense features and reveals weak objects next to bright clusters. As the cell was mounted in an aqueous buffer and recorded with water-immersion lenses, the results indicate that the optical conditions for obtaining subdiffraction resolution can be met in live cells as well[58].

by the same factor of 3–7; this is likely to become important in protein interaction studies.

The otherwise very effective lobe-reducing measures of confocalization and two-photon excitation are to some extent restrictive. Clearly, nonconfocal wide-field detection and regular illumination would make 4Pi microscopy more versatile. Therefore, the related approach of I^5M (refs. 16,19,45,46) confines itself to using the simultaneous interference of both the excitation and the (Stokes-shifted) fluorescence wavefront pairs. Impressive work has demonstrated that this method yields three-dimensional images of actin filaments with slightly better than 100-nm axial resolution in fixed cells[19]. To remove the side-lobe artifacts, I^5M-recorded data are deconvoluted offline with a linear mathematical filter.

The benefits of I^5M are readily stated: single photon excitation with arguably less photobleaching, an additional 20–50% gain in fluorescence signal, and lower cost. However, the relaxation of the side-lobe suppression comes at the expense of increased vulnerability to sample-induced aberrations, especially with nonsparse objects[37,47]. Thus I^5M imaging, which has so far relied on oil-immersion lenses, has required mounting of the cell in a medium with $n = 1.5$ (ref. 19). Live cells inevitably necessitate aqueous media ($n = 1.34$). Moreover, water-immersion lenses have a poorer focusing angle and therefore larger lobes to begin with[43]. Potential strategies for improving the tolerance of I^5M are the implementation of a nonlinear excitation mode and the combination with pseudo-confocal or patterned illumination[48]. Although these measures again add physical complexity, they may have the potential to render I^5M more suitable for live cells.

Up to now, however, live cell imaging has been the prerogative of two-photon 4Pi confocal microscopy. Recently, confocalization, two-photon excitation, and the use of excitation/fluorescence wavelength disparities have been synergistically implemented in a compact 4Pi unit that was interlaced with a state-of-the-art confocal scanning microscope (Leica TCS-SP2 AOBS, Mannheim, Germany). Consequently, a sevenfold-improved axial resolution (80 nm) over confocal microscopy has been achieved in live cell imaging, with a rugged system (unpublished data).

Lateral resolution improvement

In theory, the resolution of a confocal microscope slightly surpasses that of the standard epifluorescence microscope. Confocal fluorescence microscopes feature an effective focal spot that is narrower by 40%, and their optical transfer function (OTF) has twice the bandwidth[3]. This is because in a confocal microscope the focusing ability of the objective lens is used twice: first for focusing the excitation light onto a spot on the sample, and second for focusing the fluorescence onto a point-like detector[3]. Thus, in contrast to epifluorescence microscopy, confocal microscopy illuminates and detects selectively in space. As spatially selected detection is achieved by a pinhole, some photons are discarded, meaning that the slight improvement of resolution is gained by losing some of the light, not only from above and below the focal plane, but also from the focal plane itself. This is disadvantageous if one wishes to use the additional higher frequencies for resolution improvement through deconvolution (**Box 1**).

However, spatially selected detection can also be performed with a camera[49,50], in which case all photons are detected. Provided that they are properly reassigned, they may all contribute to the image. Therefore, in the 1980s and early 1990s, the groups of Bertero and

Box 1 The concept of resolution

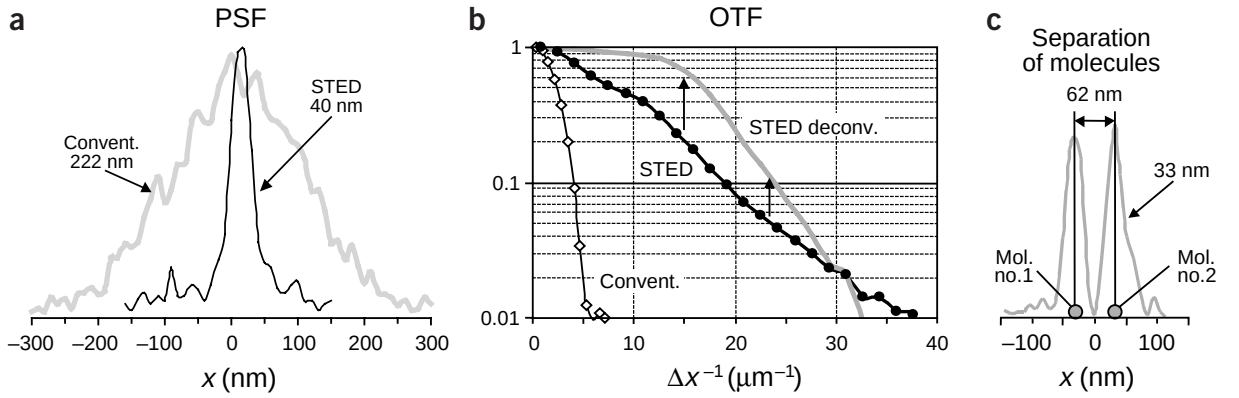

Figure 4 Quantifying resolution. (**a**) The intensity profile of the effective point-spread-function (PSF) quantifies the focal blur in the microscope. Identical fluorescent objects that are closer than the FWHM of the PSF cannot be distinguished. (**b**) The optical transfer function (OTF) is an equivalent representation of the resolution, giving the bandwidth of the spatial frequencies passed to the image; the broader the OTF, the better the resolution. The data plotted in (**a,b**) are gained by probing the fluorescent spot of a scanning microscope with a single molecule of the fluorophore JA 26, both in the conventional (Abbe type) mode and with STED. Employed conditions: $n = 1.5$, $\alpha = 67°$, wavelengths λ: 635 nm (excitation), 650 –720 nm (fluorescence collection), and 790 nm (STED). Note the 5.5-fold sharper PSF (**a**) and the equally broader OTF (**b**) of STED compared to the diffraction-limited conventional microscope. (**b**) Linear deconvolution is equivalent to multiplying the higher frequencies of the OTF that are not masked by noise (see arrows). (**c**) Subdiffraction resolution with STED microscopy. Two identical molecules located in the focal plane that are only 62 nm apart can be entirely separated by their intensity profile in the image. A similarly clear separation by conventional microscopy would require the molecules to be at least 300 nm apart. Data adapted from ref. 32.

Light microscopy resolution can be described either in real space or in spatial frequencies. In real space, the resolution is assessed by the full-width half-maximum (FWHM) of the focal spot, referred to as the point-spread function (PSF). Loosely speaking, if identical molecules are within the FWHM distance, the molecules cannot be separated in the image. Therefore, improving the resolution is equivalent to reducing the FWHM of the PSF. In a conventional microscope, the FWHM of the PSF is about $\lambda/(2n \sin \alpha)$, with λ denoting the wavelength, n the refractive index and α the semiaperture angle of the lens. **Figure 4a** shows the measured profile of the PSF in the focal plane (x) for a conventional fluorescence microscope along with its sharper subdiffraction STED fluorescence counterpart. Note the 5.5-fold improvement of resolution with STED.

In the frequency world, the sample is described as being composed of spatial frequencies. Therefore, the microscope's resolution is given by the OTF describing the strength with which these frequencies are transferred to the image[3,68]. Thus, the resolution limit is given by the highest frequency passed. PSF and OTF are intertwined by Fourier mathematics: the sharper the PSF, the broader the OTF.

Figure 4b shows the OTF of a conventional microscope along with the approximately fivefold-enlarged OTF of the STED fluorescence microscope. The marked bandwidth enlargement over that of the conventional microscope signifies a fundamental breaking of Abbe's diffraction barrier in the focal plane in the case of STED.

The FWHM of the PSF and the bandwidth of the OTF of the microscope are just estimates; a thorough description of the resolution requires the complete functions. Moreover, knowing these functions in full also makes it possible to improve the resolution by deconvolution. Note that the OTF falls off with larger spatial frequencies (**Fig. 4b**). Provided that in the image these frequencies are not swamped by noise, they can be artificially elevated by multiplication (see arrows). Mathematically, this amounts to a (de)convolution in real space. As the higher frequencies are responsible for small details in the image, deconvolution results in a further image sharpening.

As an example of linearly deconvoluted STED microscopy, two molecules at 62 nm distance are distinguished in full by two sharp peaks (**Fig. 4c**)[32]. The individual peaks are sharper (33 nm) than the initial peak of 40 nm, as a result of deconvolution. The effective OTF after deconvolution is slightly augmented at lower frequencies, as indicated by the arrows in **Figure 4b**.

Pike proposed concepts using (camera-based) spatially weighted detection in conjunction with scanning point-like illumination[49,51,52]. However, the combination of computation with scanned point-like illumination rendered these systems not very effective.

Therefore, it was not until Gustafsson recently implemented high-frequency line-patterned illumination that this approach has been brought to fruition[48]. Wide-field camera detection allows fast data acquisition, except that the pattern needs to be scanned and rotated. Because it targets the high object frequencies with the line pattern and features a somewhat improved signal, this approach has the prerequisites to yield the lateral resolution promised by ideal confocal microscopy (~100 nm). Sequential pattern alteration combined with data processing may render it more prone to movement artifacts. Thus far, superior images of the actin cytoskeleton (**Fig. 2**) have been achieved in fixed cells[48], but the coming years will show whether this method will be applicable to live cells as well.

Breaking the diffraction barrier

Confocal and related imaging modalities may, in the ideal case, surpass the diffraction barrier by a factor of two, but they do not break it. Breaking implies the potential of featuring an infinitely sharp focal spot, or an infinitely large OTF bandwidth (**Box 1**).

In 1994, together with Jan Wichmann, I published a theoretical paper that detailed a concept to eliminate the resolution-limiting effect of diffraction without eliminating diffraction itself[27]. It was termed stimulated emission depletion (STED) microscopy because the depletion of the molecular fluorescent state through stimulated emission was exploited. Shortly after, together with Mathias Kroug, I proposed ground-state depletion microscopy as a further concept with molecular resolution potential[28]. Both apply the same principle to break Abbe's barrier: a focal intensity distribution with a zero-point in space effects a saturated depletion of a molecular state that is essential to the fluorescence process[28,29]. As any saturable process is a potential candidate[29,31,53], the choice of process is solely determined by practical conditions, such as the required intensities, available light sources, photobleaching and, with respect to applications in cell biology, compatibility with live cell imaging. **Box 2** discusses the principles of this radically different approach to overcoming the diffraction barrier.

STED microscopy is a special case of this approach (**Box 3**). The fluorophore in the fluorescent state S_1 (state A) is stimulated to the ground state S_0 (state B) with a doughnut-shaped beam. Saturated depletion of S_1 confines fluorescence to the central naught. With typical I^{sat} ranging from 1 to 100 MW/cm^2, saturation factors up to $\varsigma \approx 120$ have been reported[54,55]. Doughnut imperfections have so far confined the up to tenfold possible improvement to a five- to sevenfold observed improvement over the diffraction barrier[55] (**Box 1**). Using STED wavelengths of $\lambda = 750$–800 nm, a lateral resolution of up to 28 nm has been reached in experiments with single molecules[32].

My laboratory has obtained subdiffraction images with threefold axial and doubled lateral resolution with membrane-labeled bacteria and live budding yeast cells[54]. Although there is preliminary evidence

Box 2 The principles of breaking the diffraction barrier

The basic idea underlying stimulated emission and ground state depletion microscopy can be generalized as follows. Let us assume two arbitrary fluorophore states A and B between which the molecule can be transferred; typical examples are the ground and an excited state or conformational and isomeric states. Transition A→B is induced by light, but no restriction is made on transition B→A. It may be spontaneous, but also be effected by light, heat, and so on. The only further assumption is that at least one of the states is critical to molecular fluorescence.

By denoting the rates of A→B and B→A by k_{AB} and k_{BA}, respectively, changes of the normalized populations N_A and N_B are subject to the relationship $dN_A/dt = -k_{AB}N_A + k_{BA}N_B = -dN_B/dt$. If the molecule first resides in A, or any other state, after $t \approx 5(k_{AB} + k_{BA})^{-1}$, the equilibrium population of state A is $N_A^{\infty} = k_{BA}/(k_{AB} + k_{BA})$.

We are now interested in depleting state A by light via the transition A→B, whose rate is given by $k_{AB} = \sigma I$, with σ and I denoting the molecular cross section and the photon flux per unit area, respectively. Hence, the equilibrium population is $N_A^{\infty} = k_{BA}/(\sigma I + k_{BA})$. If $I >> I^{sat} = k_{BA}/\sigma$, it follows that $N_A^{\infty} \to 0$, that is, all the molecules end up in B. I^{sat} is referred to as the saturation intensity. (We note that if A decays with k_{AB} to B, $I^{sat} = k_{AB}/\sigma$.)

If we now elect a spatial intensity distribution $I(\vec{r}) >> I^{sat}$ with a naught at $\vec{r}_0$, all molecules end up in B, except for those at $\vec{r}_0$. Thus we can create arbitrarily sharp regions of state A (**Fig. 5**). Written more formally, $I(\vec{r}) = I^{max} f(\vec{r})$, where $f(\vec{r})$ is a diffraction-limited spatial function featuring $f(\vec{r}_0) = 0$. For $I^{max} \to \infty$, the region in which the molecule can be found in A is squeezed to a point regardless of the details of $f(\vec{r})$.

If I^{max} and I^{sat} are finite, the details of $f(\vec{r})$ cannot be neglected. For example, the minima of a standing wave $f(x) = \sin^2(2\pi n x/\lambda)$ create regions of A with an FWHM of

$$\Delta x = \frac{\lambda}{\pi n} \arcsin\left(\sqrt{\frac{k_{BA}}{\sigma I_{max}}}\right) \approx \frac{\lambda}{\pi n \sqrt{\varsigma}} \qquad (1)$$

$\varsigma = I^{max}/I^{sat}$ denotes the saturation factor. $\varsigma = 1{,}000$ yields $\Delta x \approx \lambda/(100n)$, but in principle the spot of 'A molecules' can be continuously squeezed by increasing ς.

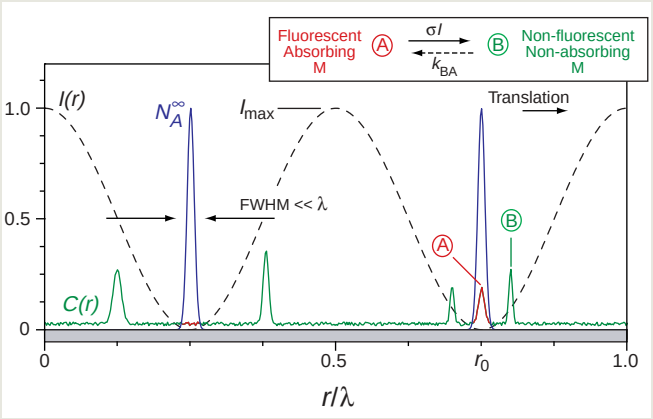

Figure 5 Diffraction-unlimited spatial resolution with a reversible, saturable optical transition: the principle. A standing wave of intensity $I(r)$ and wavelength λ is used for photoswitching molecules from state A into a state B. If only a small fraction of the total intensity I^{max} is sufficient for transferring the molecule to B, the probability $N_A^{\infty}(r)$ of finding it in A is confined to the nodal points (blue). If state A, but not B, is involved in fluorescence the signal originates from the narrow region defined by $N_A^{\infty}(r)$ only. This simple concept enables fluorescence imaging with diffraction-unlimited resolution. For this purpose, one or several nodes are scanned across the sample $C(r)$. Except for the nodes, the molecules are transiently transferred to B, so that the fluorescence from the molecules in A maps out the object $C(r)$. The FWHM and thus the resolution are determined solely by the 'saturation factor', that is, the factor by which I^{max} surpasses the required intensity threshold at which, say, 50% or more of the molecules are already in the nonfluorescent state B. The idea is readily extended to all directions in space and thus to three-dimensional imaging. Conventional camera-based detection is possible if the nodes are farther apart than the classical resolution limit of the microscope. Complete depletion of A is not required. It is sufficient that the non-nodal region features a large enough population B, so that it can be distinguished from its sharp counterpart. If not A but B is the fluorescent state, one reads out B and may obtain the same super-resolved image after subtraction.

The sharp regions of A can be used to map out the fluorophores with arbitrary resolution, as explained in **Figure 5**.

Box 3 Stimulated emission depletion microscopy

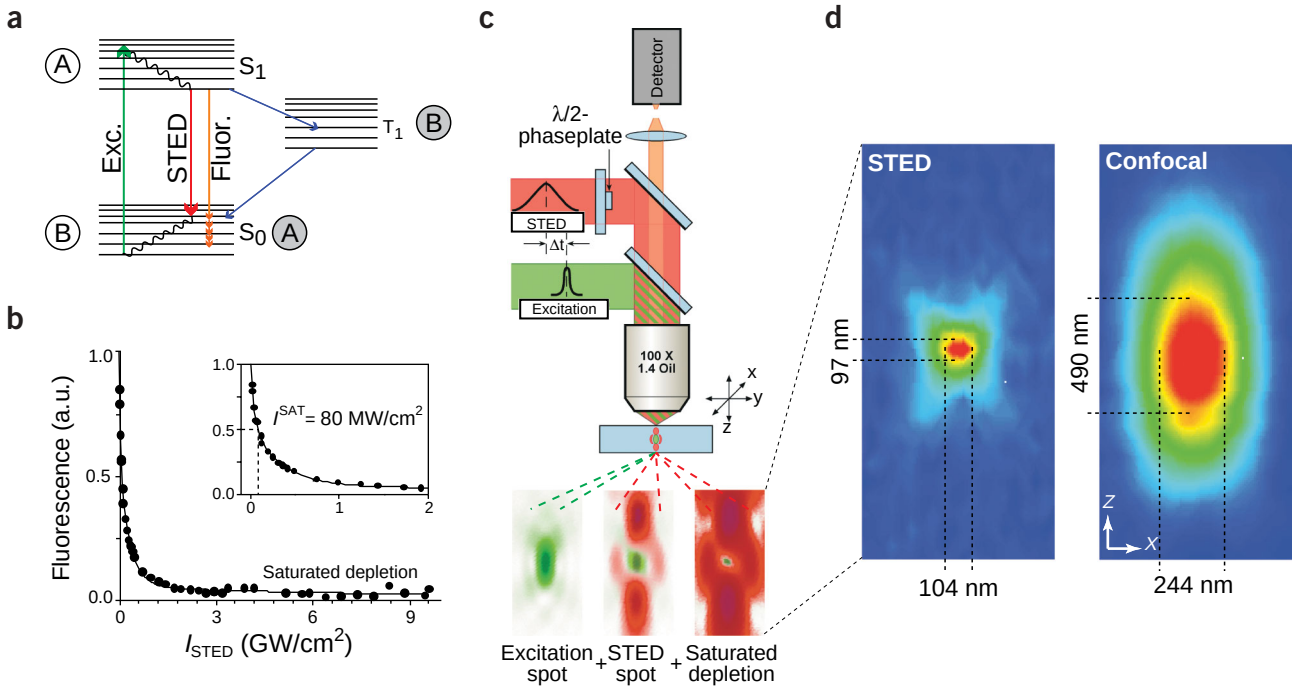

Figure 6 Physical conditions, setup and typical focal spot for STED. (**a**) Energy diagram of an organic fluorophore. Molecules in the excited state S_1 return to the ground state S_0 by spontaneous fluorescence emission. Return to S_0 may also be enforced by light through stimulated emission[67], a phenomenon with the same cross section and intensity dependence as normal absorption. To prevail over the spontaneous return, STED requires intense light pulses with duration of a fraction of the S_1 lifetime. Tuning the STED wavelength to the red edge of the emission spectrum prevents re-excitation by the same pulses. T_1 is a dark triplet state that can be accessed through S_1 and then returns to S_0 within 1–10^4 μs. (**b**) Saturated depletion of the S_1 with increasing STED pulse intensity I_{STED}, as measured by the remaining fluorescence of an organic fluorophore. Depletion of the S_1 saturates with increasing I_{STED} and therefore establishes a nonlinear relationship between the fluorescence and the intensity applied for STED. The saturation is the essential element for the breaking of the diffraction barrier, as explained in **Box 2**; the inset highlights the saturation intensity I^{sat}. (**c**) Sketch of a point-scanning STED microscope. Excitation and STED are accomplished with synchronized laser pulses focused by a lens into the sample, sketched as green and red beams, respectively. Fluorescence is registered by a detector. Below, note the panels outlining the corresponding spots at the focal plane: the excitation spot (left) is overlapped with the STED spot featuring a central naught (center). Saturated depletion by the STED beam reduces the region of excited molecules (right) to the very zero point, leaving a fluorescent spot of subdiffraction dimensions shown in panel **d**. (**d**) Fluorescent spot in the STED and in the confocal microscope. Note the doubled lateral and fivefold-improved axial resolution. The reduction in dimensions (*x*,*y*,*z*) yields an ultrasmall volume of subdiffraction size, here 0.67 attoliter[54], corresponding to 6% of its confocal counterpart. The spot size is not limited on principle but by practical circumstances such as the quality of the naught and the saturation factor of depletion.

STED microscopy produces subdiffraction resolution and subdiffraction-sized fluorescence volumes through the saturated depletion of the fluorescent state of the dye.

The nonlinear intensity dependence brought about by saturation is radically different from the nonlinearity connected with, for example, *m*-photon excitation, m^{th} harmonics generation and coherent anti-Stokes-Raman scattering[2,66]. In the last two cases, the nonlinear signal stems from the simultaneous action of more than one photon at the sample, which would only work at high focal intensities. In contrast, the nonlinearity brought about by saturation and depletion stems from a change in the population of the involved states, which is effected by a single-photon process, namely stimulated emission. Therefore, unlike in *m*-photon processes, strong nonlinearities are achieved at comparatively low intensities.

Ultrasmall volumes of detection are critical to several sensitive bioanalytical techniques. For example, fluorescence correlation spectroscopy[69] relies on small focal volumes to detect rare molecular species or interactions in concentrated solutions[70,71]. Although volume reduction can be obtained by nanofabricated structures[72], STED may prove instrumental to attaining spherical volumes at the nanoscale. Published results imply the possibility of a further decrease of the volume by another order of magnitude[53,55]. Initial applications may be hampered by the requirement of an additional pulsed laser that is tuned to the red edge of the emission spectrum of the dye. Nevertheless, STED is so far the only known method to squeeze a fluorescence volume to the zeptoliter scale without mechanical contact. Ultrasmall volumes with dimensions tens of nanometers in diameter created by STED may provide a pathway to improving the sensitivity of fluorescence-based bioanalytical techniques[73,74].

for increased nonlinear photobleaching of certain markers with the elevated intensities[56], there is no indication that the intensities applied currently would exclude the imaging of live cells. This is not surprising as the intensities are lower by two to three orders of magnitude than those used in multiphoton microscopy[4]. Moreover, STED has proved to be sensitive to single molecules, despite the proximity of the STED wavelength to the emission peak. In fact, my group has been able to switch individual molecules on and off by STED on command[57].

The power of STED and 4Pi microscopy has been synergistically combined[29] to demonstrate the first axial resolution of 30–40 nm in focusing light microscopy[53]. Initial studies in my laboratory have enabled *xz* images of membrane-labeled bacteria to be obtained[53]. More recent studies are extending STED-4Pi microscopy to immunofluorescence imaging[58]. In this work, we have demonstrated a spatial resolution of ~50 nm in the imaging of the microtubular meshwork of a mammalian cell (**Fig. 3**). These results indicate that the basic physical hurdles have been overcome in attaining a three-dimensional resolution to the order of a few tens of nanometers. Because the samples were mounted in an aqueous buffer[53,58], the results indicate that the optical conditions for obtaining subdiffraction resolution are met under the physical conditions encountered in live cell imaging.

STED microscopy is still at an early stage of development. Our work[57] has demonstrated the suitability of laser diodes for both excitation and depletion, but further efforts are required to implement STED into fast-scanning systems. The lack of compact tunable pulsed light sources in the visible range has so far confined STED investigations to red-emitting dyes. As more efficient light sources become available, however, both visible blue, green and yellow fluorophores as well as fluorescent proteins will be interesting candidates for saturated depletion[59,60]. Shorter wavelengths will also lead to higher spatial resolution. However, a further increase of the intensity might be barred in aqueous media by intolerable photobleaching. Although STED pulses >300 ps recently improved dye photostability[56], saturation factors (ς) of >200 might not be readily attainable.

Fortunately, this limitation can be counteracted by lowering I^{sat} through k_{BA} (**Box 2**). Thus, it has been proposed to deplete the ground state (now state A) by targeting an excited state (B) with a comparatively long lifetime[28,29], such as the metastable triplet state T_1 (**Fig. 6a**). In many fluorophores, T_1 can be reached through the S_1 with a quantum efficiency of 1–10%[61]. A forbidden transition, the relaxation of the T_1 is 10^3- to 10^5-fold slower than that of the S_1, thus giving I^{sat}_{AB} = 0.1–100 kW/cm^2. The signal to be measured (from the naught) is the fluorescence of the molecules that remained in the singlet system, through a synchronized further excitation[28]. The disadvantage here is the involvement of the T_1 in photobleaching. Potential alternatives are metastable states of rare earth metal ions that are fed through chelates.

Another option is to deplete the S_0 by saturating the S_1 (now B), as has been proposed recently[30]. This is perhaps the simplest realization of saturated depletion because it requires just excitation wavelength matching (**Fig. 6**). However, as the fluorescence emission maps the spatially extended 'majority population' in state B, the superresolved images (represented by state A) are hidden under a bright signal from B (**Box 2**). Thus, acquiring these images requires computational extraction, which makes this approach prone to noise, unless the sample is very sparse. Nevertheless, the simplicity of raw data acquisition may render it attractive for the imaging of fixed cells. I^{sat} is of the same order as with STED, because the saturation of fluorescence also competes against the spontaneous decay of S_1. Therefore attaining $\varsigma > 200$ might involve similar photostability issues.

Importantly, the quest for large ς at low I^{sat} should be solved by compounds with two (semi-) stable states[31,58]. If the rate k_{BA} (and the spontaneous rate k_{AB}) almost vanishes, large ς values are attained at low intensities. The lowest useful intensity is set by the concomitant increase in switching time. In the ideal case, the marker is a bistable fluorescent compound that can be photoswitched, at separate wavelengths, from a fluorescent state to a dark state, and vice versa. A photoswitchable coupled molecular system, based on a photochromic diarylethene derivative and a fluorophore, has been reported[62]. Using equation (1), one can determine that focusing less than 100 μW of deep-blue 'switch-off light' to an area of 10^{-8} cm^2 for 50 μs should yield better than 5-nm spatial resolution. Targeted optimization of photochromic or other compounds toward fatigue-free switching and visible light operation could therefore open up radically new avenues in microscopy and data storage[31].

For live cell imaging, fluorescent proteins are more advantageous. Any fluorescent protein that can be pushed to a dark state[29,31] (and vice versa), and has a lifetime longer than 10 ns, may result in larger ς; however, fluorescent proteins that can be switched 'on' and 'off' at different wavelengths are a more attractive option[31]. An example is *Anemonia sulcata* purple protein (asFP595), which, according to the published data[63], may allow saturated depletion of the fluorescence state with intensities of less than a few watts per square centimeter. Under favorable switching conditions, such or similar fluorescent proteins should allow a spatial resolution of better than 10 nm[31] at very low intensities. The low power involved should also enable parallelization of saturation through an array of minima or dark lines. Initial realization of very low intensity depletion microscopes may, however, be challenged by switching fatigue[62] and overlapping action spectra[63]. However, the prospect of attaining nanoscale resolution with regular lenses and focused light is an incentive to surmount these challenges by strategic fluorophore modification[31].

Conclusions

Although most textbooks still portray light microscopy as limited by resolution, in recent years concepts have emerged that are poised to radically change this view. Featuring the aperture angle of two opposing lenses, 4Pi and its widefield cousin I^{5}M microscopy have displayed 80–100 nm resolution along the optic axis. In particular, compact 4Pi confocal microscopes are emerging that feature the same scanning and detection amenities as commercial confocal systems, but with a sevenfold improved optical sectioning in live cells.

Moreover, we have begun to map out concrete physical concepts for overcoming the resolution limit altogether. By exploiting these concepts, my group has been able to break the diffraction barrier in several imaging experiments[64], including experiments with single fluorescent molecules, simple fixed specimens and live biological specimens. STED microscopy has so far witnessed a resolution improvement by up to a factor of 6, resulting in the smallest fluorescent volumes that have been created with focused light so far. Combined with 4Pi-microscopy, STED has provided the first demonstration of immunofluorescence imaging with an (axial) resolution of 50 nm, and this value is more of a starting point than a limit. Future research on its spectroscopy conditions and on practical aspects[65] will reveal its full potential.

Relying on saturated optical transitions, the spatial resolution of the new concepts is determined by the attainable saturation level. The nonlinear intensity dependence brought about by saturation is fundamentally different from the nonlinearity connected with *m*-photon excitation, or with m^{th} harmonics generation, coherent anti-Stokes-Raman scattering[2,66], etc. In the latter cases, the nonlinear signal stems from the action of more than one photon at the sample at the same time, which demands high focal intensities. In contrast, the nonlinear-

ity brought about by saturation and depletion stems from a change in the population of the involved states, which opens the door to low-intensity implementations. I expect this detail to be essential to opening up the cellular nanoscale with visible light and regular lenses. Because of their population kinetics, switchable dyes and fluorescent proteins should allow high levels of saturation at low light intensities[31]. Although first candidates have been named, dedicated synthesis or protein engineering might uncover a whole new range of suitable markers.

Physics undoubtedly has greatly contributed to the emergence of molecular and cell biology in the past century. Paradoxically, the development of nanoscale imaging with focused light in molecular and cell biology might now topple a longstanding paradigm of physics.

ACKNOWLEDGMENTS

I thank M. Dyba, A. Egner, S. Jakobs, J. Jethwa, L. Kastrup, J. Keller and A. Schönle for constructive reading. The work of this laboratory has been funded by the Max Planck Society, with further support by the German Ministry of Research and Education, the Deutsche Forschungsgemeinschaft, and the Volkswagen Foundation.

COMPETING INTERESTS STATEMENT

The author declares that he has no competing financial interests.

Published online at http://www.nature.com/naturebiotechnology/

1. Abbe, E. Beiträge zur Theorie des Mikroskops und der mikroskopischen Wahrnehmung. *Arch. Mikroskop. Anat.* **9**, 413–420 (1873).
2. Sheppard, C.J.R. & Kompfner, R. Resonant scanning optical microscope. *Appl. Opt.* **17**, 2879–2882 (1978).
3. Wilson, T. & Sheppard, C.J.R. *Theory and Practice of Scanning Optical Microscopy* (Academic Press, New York, 1984).
4. Denk, W., Strickler, J.H. & Webb, W.W. Two-photon laser scanning fluorescence microscopy. *Science* **248**, 73–76 (1990).
5. Pawley, J. Handbook of Biological Confocal Microscopy (Plenum, New York, 1995).
6. Basché, T., Moerner, W.E., Orrit, M. & Wild, U.P. *Single-Molecule Optical Detection, Imaging and Spectroscopy* (VCH, Weinheim, New York, Basel, Tokyo, 1997).
7. Weiss, S. Fluorescence spectroscopy of single biomolecules. *Science* **283**, 1676–1683 (1999).
8. Ha, T., Enderle, T., Chemla, D.S. & Weiss, S. Dual-molecule spectroscopy: molecular rulers for the study of biological macromolecules. *IEEE J. Select. Top. Quantum Electron.* **2**, 1115–1128 (1996).
9. Bornfleth, H., Sätzler, K., Eils, R. & Cremer, C. High-precision distance measurements and volume-conserving segmentation of objects near and below the resolution limit in three-dimensional confocal fluorescence microscopy. *J. Microsc.* **189**, 118–136 (1998).
10. Oijen, M.v., Köhler, J., Schmidt, J., Müller, M. & Brakenhoff, G.J. 3-Dimensional super-resolution by spectrally selective imaging. *Chem. Phys. Lett.* **292**, 183–187 (1998).
11. Lacoste, T.D. *et al.* Ultrahigh-resolution multicolor colocalization of single fluorescent probes. *Proc. Natl. Acad. Sci. USA* **97**, 9461–9466 (2000).
12. Hettich, C. *et al.* Nanometer resolution and coherent optical dipole coupling of two individual molecules. *Science* **298**, 385–389 (2002).
13. Born, M. & Wolf, E. *Principles of Optics* 6th edn. (Pergamon, Oxford, 1993).
14. Hell, S.W. Double-confocal microscope. European Patent 0491289 (1990).
15. Hell, S. & Stelzer, E.H.K. Properties of a 4Pi-confocal fluorescence microscope. *J. Opt. Soc. Am. A* **9**, 2159–2166 (1992).
16. Gustafsson, M.G.L., Agard, D.A. & Sedat, J.W. Sevenfold improvement of axial resolution in 3D widefield microscopy using two objective lenses. *Proc. Soc. Photo-Optical Instrumentation Engineers* **2412**, 147–156 (1995).
17. Hell, S.W. & Stelzer, E.H.K. Fundamental improvement of resolution with a 4Pi-confocal fluorescence microscope using two-photon excitation. *Opt. Commun.* **93**, 277–282 (1992).
18. Egner, A., Jakobs, S. & Hell, S.W. Fast 100-nm resolution 3D-microscope reveals structural plasticity of mitochondria in live yeast. *Proc. Natl. Acad. Sci. USA* **99**, 3370–3375 (2002).
19. Gustafsson, M.G.L., Agard, D.A. & Sedat, J.W. I5M: 3D widefield light microscopy with better than 100 nm axial resolution. *J. Microsc.* **195**, 10–16 (1999).
20. Pohl, D.W. & Courjon, D. *Near Field Optics* (Kluwer, Dordrecht, 1993).
21. Toraldo di Francia, G. Supergain antennas and optical resolving power. *Nuovo Cimento Suppl.* **9**, 426–435 (1952).
22. Lukosz, W. Optical systems with resolving powers exceeding the classical limit. *J. Opt. Soc. Am.* **56**, 1463–1472 (1966).
23. Xu, C., Zipfel, W., Shear, J.B., Williams, R.M. & Webb, W.W. Multiphoton fluorescence excitation: new spectral windows for biological nonlinear microscopy. *Proc. Natl. Acad. Sci. USA* **93**, 10763–10768 (1996).
24. Hänninen, P.E., Lehtelä, L. & Hell, S.W. Two- and multiphoton excitation of conjugate dyes with continuous wave lasers. *Opt. Commun.* **130**, 29–33 (1996).
25. Schönle, A., Hänninen, P.E. & Hell, S.W. Nonlinear fluorescence through intermolecular energy transfer and resolution increase in fluorescence microscopy. *Ann. Phys. (Leipzig)* **8**, 115–133 (1999).
26. Schönle, A. & Hell, S.W. Far-field fluorescence microscopy with repetitive excitation. *Eur. Phys. J. D* **6**, 283–290 (1999).
27. Hell, S.W. & Wichmann, J. Breaking the diffraction resolution limit by stimulated emission: stimulated emission depletion microscopy. *Opt. Lett.* **19**, 780–782 (1994).
28. Hell, S.W. & Kroug, M. Ground-state depletion fluorescence microscopy, a concept for breaking the diffraction resolution limit. *Appl. Phys. B* **60**, 495–497 (1995).
29. Hell, S.W. in Increasing the resolution of far-field fluorescence light microscopy by point-spread-function engineering in *Topics in Fluorescence Spectroscopy* Vol. 5. (ed. Lakowicz, J.R.) 361–422 (Plenum, New York, 1997).
30. Heintzmann, R., Jovin, T.M. & Cremer, C. Saturated patterned excitation microscopy—a concept for optical resolution improvement. *J. Opt. Soc. Am. A* **19**, 1599–1609 (2002).
31. Hell, S.W., Jakobs, S. & Kastrup, L. Imaging and writing at the nanoscale with focused visible light through saturable optical transitions. *Appl. Phys. A* **77**, 859–860 (2003).
32. Westphal, V., Kastrup, L. & Hell, S.W. Lateral resolution of 28nm (λ/25) in far-field fluorescence microscopy. *Appl. Phys. B* **77**, 377–380 (2003).
33. Lanni, F. Applications of Fluorescence in the Biomedical Sciences 1st edn. (Liss, New York, 1986).
34. Bailey, B., Farkas, D.L., Taylor, D.L. & Lanni, F. Enhancement of axial resolution in fluorescence microscopy by standing-wave excitation. *Nature* **366**, 44–48 (1993).
35. Schrader, M. & Hell, S.W. 4Pi-confocal images with axial superresolution. *J. Microsc.* **183**, 189–193 (1996).
36. Hell, S.W., Schrader, M. & van der Voort, H.T.M. Far-field fluorescence microscopy with three-dimensional resolution in the 100 nm range. *J. Microsc.* **185**, 1–5 (1997).
37. Nagorni, M. & Hell, S.W. Coherent use of opposing lenses for axial resolution increase in fluorescence microscopy. I. Comparative study of concepts. *J. Opt. Soc. Am. A* **18**, 36–48 (2001).
38. Holmes, T.J. Maximum-likelihood image restoration adapted for non-coherent optical imaging. *J. Opt. Soc. Am. A* **5**, 666–673 (1988).
39. Carrington, W.A. *et al.* Superresolution in three-dimensional images of fluorescence in cells with minimal light exposure. *Science* **268**, 1483–1487 (1995).
40. Holmes, T.J. *et al.* Light microscopic images reconstructed by maximum likelihood deconvolution in *Handbook of Biological Confocal Microscopy* (ed. Pawley, J.) 389–400 (Plenum, New York, 1995).
41. Nagorni, M. & Hell, S.W. 4Pi-confocal microscopy provides three-dimensional images of the microtubule network with 100- to 150-nm resolution. *J. Struct. Biol.* **123**, 236–247 (1998).
42. Hell, S.W. & Nagorni, M. 4Pi confocal microscopy with alternate interference. *Optics Lett.* **23**, 1567–1569 (1998).
43. Bahlmann, K., Jakobs, S. & Hell, S.W. 4Pi-confocal microscopy of live cells. *Ultramicroscopy* **87**, 155–164 (2001).
44. Egner, A., Goroshkov, A., Verrier, S., Söling, H.-D. & Hell, S.W. Golgi apparatus of live mammalian cell at 100 nm resolution. *J. Struct. Biol.* in the press (2003).
45. Gustafsson, M.G., Agard, D.A. & Sedat, J.W. 3D widefield microscopy with two objective lenses: experimental verification of improved axial resolution. in *Three-Dimensional Microscopy: Image Acquisition and Processing III* (eds. Cogswell, C., Kino, G.S. & Wilson, T.) 62–66 (SPIE, New York, 1996).
46. Gustafsson, M.G.L. Extended resolution fluorescence microscopy. *Curr. Opin. Struct. Biol.* **9**, 627–634 (1999).
47. Nagorni, M. & Hell, S.W. Coherent use of opposing lenses for axial resolution increase in fluorescence microscopy. II. Power and limitation of nonlinear image restoration. *J. Opt. Soc. Am. A* **18**, 49–54 (2001).
48. Gustafsson, M.G.L. Surpassing the lateral resolution limit by a factor of two using structured illumination microscopy. *J. Microsc.* **198**, 82–87 (2000).
49. Bertero, M., De Mol, C., Pike, E.R. & Walker, J.G. Resolution in diffraction-limited imaging, a singular value analysis. IV. The case of uncertain localization or non-uniform illumination of the object. *Opt. Acta* **31**, 923–946 (1984).
50. Barth, M. & Stelzer, E. Boosting the optical transfer function with a spatially resolving detector in a high numerical aperture confocal reflection microscope. *Optik* **96**, 53–58 (1994).
51. Walker, J.G. *et al.* Superresolving scanning optical microscopy using holographic optical processing. *J. Opt. Soc. Am. A* **10**, 59–64 (1993).
52. Young, M.R., Davies, R.E., Pike, E.R., Walker, J.G. & Bertero, M. Superresolution in confocal scanning microscopy: experimental confirmation in the 1D coherent case. *Europhys. Lett.* **9**, 773–778 (1989).
53. Dyba, M. & Hell, S.W. Focal spots of size λ/23 open up far-field fluorescence microscopy at 33 nm axial resolution. *Phys. Rev. Lett.* **88**, 163901 (2002).
54. Klar, T.A., Jakobs, S., Dyba, M., Egner, A. & Hell, S.W. Fluorescence microscopy with diffraction resolution limit broken by stimulated emission. *Proc. Natl. Acad. Sci. USA* **97**, 8206–8210 (2000).
55. Klar, T.A., Engel, E. & Hell, S.W. Breaking Abbe's diffraction resolution limit in fluorescence microscopy with stimulated emission depletion beams of various shapes. *Phys. Rev. E* **64**, 066613, 066611–066619 (2001).
56. Dyba, M. & Hell, S.W. Photostability of a fluorescent marker under pulsed excited–state depletion through stimulated emission. *Appl. Opt.* **42**, 5123–5129 (2003).
57. Westphal, V., Blanca, C.M., Dyba, M., Kastrup, L. & Hell, S.W. Laser-diode–stimulated emission depletion microscopy. *Appl. Phys. Lett.* **82**, 3125–3127 (2003).
58. Dyba, M., Jakobs, S. & Hell, S.W. Immunofluorescence stimulated emission depletion microscopy. *Nat. Biotechnol.* **21**, 1303–1304 (2003).

59. Gryczynski, I., Bogdanov, V. & Lakowicz, J.R. Light quenching and depolarization of fluorescence observed with laser pulses. A new experimental opportunity in time-resolved fluorescence spectroscopy. *Biophys. Chem.* **49**, 223–232 (1994).
60. Lakowicz, J.R. & Gryczynski, I. in *Topics in Fluorescence Spectroscopy* Vol. 5 (ed. Lakowicz, J.R.) 305–355 (Plenum, New York, 1997).
61. Lakowicz, J.R. *Principles of Fluorescence Spectroscopy* (Plenum, New York, 1983).
62. Irie, M., Fukaminato, T., Sasaki, T., Tamai, N. & Kawai, T. A digital fluorescent molecular photoswitch. *Nature* **420**, 759–760 (2002).
63. Lukyanov, K.A. *et al.* Natural animal coloration can be determined by a nonfluorescent green fluorescent protein homolog. *J. Biol. Chem.* **275**, 25879–25882 (2000).
64. Hänninen, P. Beyond the diffraction limit. *Nature* **419**, 802 (2002).
65. Stephens, D.J. & Allen, V.J. Light microscopy techniques for live cell imaging. *Science* **300**, 82–91 (2003).
66. Shen, Y.R. *The Principles of Nonlinear Optics* Edn. 1 (Wiley, New York, 1984).
67. Einstein, A. Zur Quantentheorie der Strahlung. *Physik. Zeitschr.* **18**, 121–128 (1917).
68. Goodman, J.W. *Introduction to Fourier Optics* (McGraw-Hill, New York, 1968).
69. Magde, D., Elson, E.L. & Webb, W.W. Thermodynamic fluctuations in a reacting system—measurement by fluorescence correlation spectroscopy. *Phys. Rev. Lett.* **29**, 705–708 (1972).
70. Eigen, M. & Rigler, R. Sorting single molecules: applications to diagnostics and evolutionary biotechnology. *Proc. Natl. Acad. Sci. USA* **91**, 5740–5747 (1994).
71. Elson, E.L. & Rigler, R. (eds.) *Fluorescence Correlation Spectroscopy. Theory and Applications* (Springer, Berlin, 2001).
72. Levene, M.J. *et al.* Zero-mode waveguides for single-molecule analysis at high concentrations. *Science* **299**, 682–686 (2003).
73. Weiss, S. Shattering the diffraction limit of light: a revolution in fluorescence microscopy? *Proc. Nat. Acad. Sc. USA* **97**, 8747–8749 (2000).
74. Laurence, T.A. & Weiss, S. How to detect weak pairs. *Science* **299**, 667–668 (2003).